

Mechanism investigation of oxidative decarboxylation catalyzed by two iron(II) and 2-oxo-glutarate dependent enzymes

Jhih-Liang Huang, Yijie Tang, Cheng-Ping Yu, Dev Sanyal,
Xinglin Jia, Xinyu Liu, Yisong Guo, and Wei-chen Chang

Biochemistry, **Just Accepted Manuscript** • DOI: 10.1021/acs.biochem.8b00115 • Publication Date (Web): 27 Feb 2018

Downloaded from <http://pubs.acs.org> on March 3, 2018

Just Accepted

“Just Accepted” manuscripts have been peer-reviewed and accepted for publication. They are posted online prior to technical editing, formatting for publication and author proofing. The American Chemical Society provides “Just Accepted” as a service to the research community to expedite the dissemination of scientific material as soon as possible after acceptance. “Just Accepted” manuscripts appear in full in PDF format accompanied by an HTML abstract. “Just Accepted” manuscripts have been fully peer reviewed, but should not be considered the official version of record. They are citable by the Digital Object Identifier (DOI®). “Just Accepted” is an optional service offered to authors. Therefore, the “Just Accepted” Web site may not include all articles that will be published in the journal. After a manuscript is technically edited and formatted, it will be removed from the “Just Accepted” Web site and published as an ASAP article. Note that technical editing may introduce minor changes to the manuscript text and/or graphics which could affect content, and all legal disclaimers and ethical guidelines that apply to the journal pertain. ACS cannot be held responsible for errors or consequences arising from the use of information contained in these “Just Accepted” manuscripts.



Mechanism investigation of oxidative decarboxylation catalyzed by two iron(II) and 2-oxo-glutarate dependent enzymes

Jih-Liang Huang,^{†&} Yijie Tang,^{‡&} Cheng-Ping Yu,[†] Dev Sanyal,[†] Xinglin Jia, Xinyu Liu,^{*,§} Yisong Guo,^{*,‡} Wei-chen Chang^{*,†}

[†]Department of Chemistry, North Carolina State University, Raleigh, North Carolina 27695, United States

[‡]Department of Chemistry, Carnegie Mellon University, Pittsburgh, Pennsylvania 15213, United States

[§]Department of Chemistry, University of Pittsburgh, Pittsburgh, Pennsylvania 15260, United States.

Supporting Information Placeholder

ABSTRACT: Two non-heme iron enzymes, IsnB and AmbI3, catalyze a novel decarboxylation-assisted olefination to produce indole vinyl isonitrile, an important building block for many natural products. Compared to other reactions catalyzed by this enzyme family, decarboxylation-assisted olefination represents an attractive biosynthetic route and a mechanistically unexplored pathway in constructing a C=C bond. Using mechanistic probes, transient kinetics, reactive intermediate trapping, spectroscopic characterizations and product analysis, we propose that both IsnB and AmbI3 initiate stereoselective olefination via a benzylic C-H bond activation by an Fe(IV)-oxo intermediate, and the reaction likely proceeds through a radical or a carbocation induced decarboxylation to complete C=C bond installation.

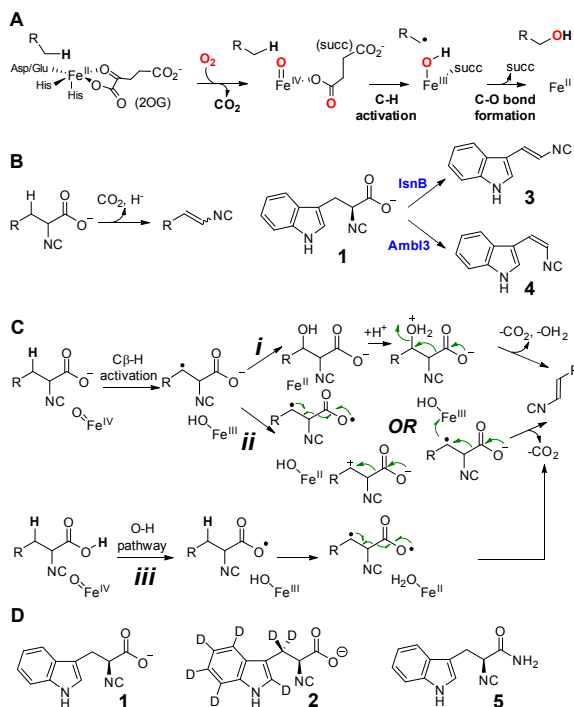
Non-heme mononuclear iron(II) and 2-oxo-glutarate-dependent (Fe/2OG) enzymes catalyze a broad range of oxidative transformations involved in the regulation and biosynthesis of cellular metabolites.^{1,2} Among these diverse transformations, the mechanism of hydroxylation has been most extensively investigated. This process is initiated by H-atom abstraction (HAT) by an Fe(IV)-oxo species, followed by a rapid C-O bond formation between the substrate radical and Fe(III)-OH species (the OH-rebound pathway, Scheme 1A).² The chemistry of several less well-studied Fe/2OG enzymes, however, does not appear to utilize the “canonical” OH-rebound mechanism. Examples of such transformations include the halogenation³⁻⁵ (e.g., CytC3, SyrB2 and WelO5), the desaturation involving cleavage of two C-H bonds^{6,7} (e.g., AsqJ and CarC), and the C-O bond formation leading to epoxide and endoperoxide^{6,8,9} (e.g., AsqJ, H6H and Ftmox1). The oxidative decarboxylation, recently found in vinyl isonitrile and ethylene production pathways, represent new types of Fe/2OG enzyme activity. Compared to ethylene production,¹⁰ the underlying reaction mechanism of vinyl isonitrile biosynthesis is poorly understood.^{11,12}

We have recently shown that the isonitrile-containing L-tryptophan precursor (**1**) is a substrate for both the *trans*-indolyl vinyl isonitrile (**3**) synthase IsnB and the *cis*-indolyl vinyl isonitrile (**4**) synthase AmbI3.¹¹⁻¹³ The stereoselective formation of **3** and **4** catalyzed by IsnB and AmbI3 is accompanied by the net loss of a hydride at the benzylic carbon of **1** and the elimination of CO₂¹¹⁻¹³ (Scheme 1B). The IsnB/AmbI3-mediated olefination is distinct from the reactions catalyzed by other Fe/2OG desaturases where the C=C bond formation involves two consecutive C-H bond cleavages.² Toward this end, several mechanistic proposals

can be formulated for IsnB/AmbI3-type desaturases. We and others have previously proposed a pathway involving HAT by a putative Fe(IV)-oxo species followed by subsequent OH-rebound to produce a hydroxylated intermediate, with dehydration assisted by decarboxylation to produce the olefin and CO₂^{13,14} (Scheme 1C, pathway *i*). On the other hand, inspired by recent mechanistic studies of Fe/2OG enzymes,^{1,2} other mechanistic possibilities can be envisioned such as those involving a substrate radical or a cation intermediate. Similar pathways have been suggested for the cytochrome P-450 enzyme, OleT,¹⁵ the non-heme iron enzyme, UndA,¹⁶ and the radical SAM dependent enzyme, MftC¹⁷ (Scheme 1C, pathway *ii*). A third possibility, although less likely, may involve a pathway that utilizes O-H bond activation followed by a C-C bond scission and a C-H bond cleavage. (Scheme 1C, pathway *iii*). To elucidate the catalytic mechanisms of IsnB and AmbI3, we prepared the substrate **1**, its deuterated analog **2**, the product standards **3** and **4**, and the amide analog **5**. IsnB and AmbI3 reactions were characterized using transient state kinetics, Mössbauer spectroscopy and liquid chromatograph coupled mass spectrometry (LC-MS).

Transient state kinetics via stopped-flow optical absorption spectroscopy (SF-Abs) were employed to reveal intermediates during the IsnB and AmbI3 catalysis. Reactions were initiated by rapid mixing of the anaerobic IsnB (or AmbI3)•Fe(II)•2OG•**1** (or **2**) complex with equal volume of oxygenated buffer at 5 °C with final concentrations of ~ 0.5 mM O₂, 0.3 mM enzyme, 0.27 mM Fe(II), 2.7 mM 2OG, and 0.68 mM substrate. The IsnB•Fe(II)•2OG•**1** complex exhibits a broad absorption band centered at ~ 540 nm which can be assigned to the Fe(II)-2OG metal-to-ligand charge transfer (MLCT) band commonly observed with Fe(II)/2OG enzymes (Fig. S6).¹⁸ After mixing, the MLCT band depletes over ~ 1 s and two stages of MLCT band decay were observed (Fig. 1a). Before 0.1 s, the absorption decreased near 600 nm with a concomitant increase in absorption near 320 nm. The isosbestic point observed at ~ 480 nm in the difference spectra suggests a conversion of the IsnB•Fe(II)•2OG•**1** complex to a reactive intermediate. We tentatively assign this intermediate as an Fe(IV)-oxo species based on similar absorption changes observed in several well-characterized Fe/2OG enzymes.^{19,20} In the second stage of MLCT decay (> 0.1 s post-mixing), the features in the 400 – 700 nm region decrease, suggesting the disappearance of the IsnB•Fe(II)•2OG•**1** and Fe(IV)-oxo complexes. Simultaneously, the absorbance at 320 nm continues to increase, which can be attributed to the formation of product **3** (Fig. S16). The negative absorption feature of the MLCT band after 1 s implies that the IsnB•Fe(II)•2OG•**1** complex

was largely depleted. The partial reformation of Fe(II)-2OG MLCT band is further observed up to 10 s, which could be attributed to the reformation of IsnB•Fe(II)•2OG complex due to the depletion of O₂ and/or substrate.



Scheme 1. (A) Schematic representation of hydroxylation catalyzed by Fe/2OG enzyme; (B) Left: decarboxylation-assisted desaturation catalyzed by IsnB, AmbI3 and other Fe/2OG enzymes. Right: outcomes of IsnB and AmbI3 catalyzed stereoselective vinyl isonitrile production; (C) Possible pathways for decarboxylation-assisted olefination; (D) Substrates and analog used in this study.

The time-dependent changes of the absorption at 400 nm (Fig. 1b) were analyzed using a two-step kinetic model (enzyme substrate complex + O₂ → Fe(IV)-oxo → enzyme product complex, see the SI for more discussion) that has been used in other Fe/2OG enzymes.¹⁹ The 320 nm trace normally selected to analyze Fe(IV)-oxo kinetics^{19,21} is not used here due to the interference of product absorption at ~320 nm (Fig. S16). The rate constants for the formation and decay of the Fe(IV)-oxo intermediate were simulated to be ~30 mM⁻¹s⁻¹ and 4.0±0.2 s⁻¹ and are similar to those of reported Fe/2OG enzymes, such as TauD, SyrB2 and CarC.^{4, 19, 21} When **2** was used, the rate of Fe(IV)-oxo formation was not perturbed (Fig. 1, S7 and S8); however, the lifetime of the Fe(IV)-oxo intermediate was greatly extended (Fig. 1b, blue trace) and did not fully decay up to ~30 s (Fig. S8). Thus, the observed rate constant for the Fe(IV)-oxo decay is reduced to 0.05±0.01 s⁻¹. When AmbI3 was examined, analogous results were obtained where the rate constants for Fe(IV)-oxo formation and decay were found to be ~55 mM⁻¹s⁻¹ and 13±1 s⁻¹ or ~55 mM⁻¹s⁻¹ and 0.25±0.05 s⁻¹ when **1** or **2** were used (Fig. S9). The greater accumulation and slow decay of the Fe(IV)-oxo species when **2** was used is likely due to the H/D kinetic isotope effect (H/D KIE of ~80 for IsnB and ~50 for AmbI3) on the C-H activation step, which has been documented in several Fe/2OG enzymes.^{2, 20, 21} Together, these results support the hypothesis that an Fe(IV)-oxo species is responsible for initiating the benzylic C-H activation in IsnB/AmbI3.

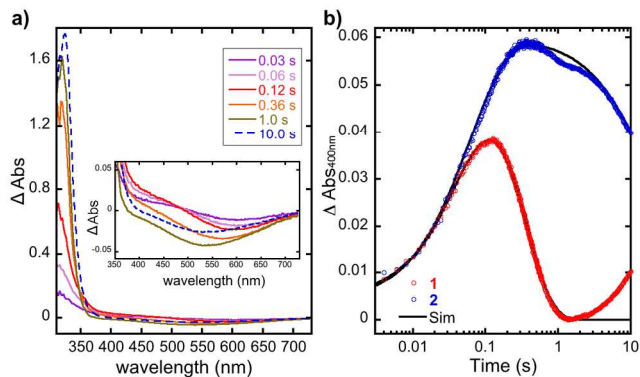


Figure 1. Kinetic evidence for the C_β-H activation in the IsnB catalysis. (A) Changes in absorbance at the indicated reaction times after mixing IsnB•Fe(II)•2OG•1 with O₂. The spectra at the indicated time points were obtained by subtracting the spectrum at 0.002 s. (B) Kinetic traces at 400 nm is used to indicate the formation and the decay of the Fe(IV)-oxo intermediate in the reactions using **1 (red) or **2** (blue), with simulations shown in black. The SF-Abs results of AmbI3 reaction are shown in Figure S9.**

To corroborate the results obtained from the SF-Abs studies, freeze-quench coupled Mössbauer experiments were performed (see the SI for more discussion). The IsnB•Fe(II)•2OG•**1** (or **2**) complex exhibited a quadrupole doublet in the Mössbauer spectrum measured at 4.2 K with isomer shift (δ) of 1.24 mm/s and a quadrupole splitting ($|\Delta E_Q|$) of 3.09 mm/s, which is typical for high-spin ferrous species (Fig. 2). In addition to this species which represents ~75% of the total iron in the sample, the remaining 25% of the iron in the sample belonged to a species exhibiting a quadrupole doublet with $\delta = 0.24$ mm/s, and $|\Delta E_Q| = 0.54$ mm/s. The high field measurement revealed that this species has a diamagnetic ground state ($S = 0$) with parameters resembling those of isonitrile-iron(II) complexes (Fig. S13, Table S3). Therefore, we reasoned that this minor species originates from the coordination of the isonitrile group of **1** to the Fe(II) center. Following addition of O₂, it remains unchanged (Table S2). Thus it is not involved in IsnB catalysis. The Mössbauer spectra of samples quenched at various time points after mixing with oxygenated buffer revealed the accumulation of an Fe(IV)-oxo intermediate, which is evidenced by the observation of a quadrupole doublet with $\delta = 0.31$ mm/s, and $|\Delta E_Q| = 0.92$ mm/s. The Fe(IV)-oxo species accumulated to a maximum of ~28% of the total iron in the sample quenched at 0.13 s and decayed to less than 4% at 1 s. In addition, a quadrupole doublet representing another high-spin ferrous species with $\delta = 1.15$ mm/s, and $|\Delta E_Q| = 3.24$ mm/s, was formed in concomitance with the decay of the Fe(IV)-oxo species. This quadrupole doublet is different from the substrate bound complex and likely represents the IsnB-Fe(II)-product complex. When **2** was used, the amount of Fe(IV)-oxo species observed at 0.03 s was similar (~25%) with that in the case of **1**; however, it accumulated to a higher level (~45%) at 0.13 s, and hardly decayed at 1 s. In a sample quenched at 10 s, the Fe(IV)-oxo species still accounted for ~20% of the total iron. These observations are consistent with the SF-Abs experiments results that a large H/D KIE is observed on the decay of the Fe(IV)-oxo species (Fig. S10).

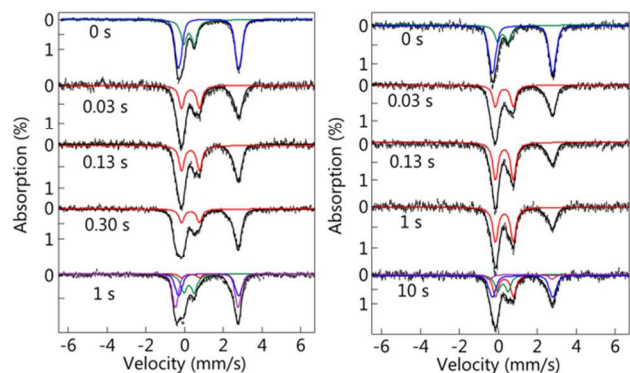


Figure 2. 4.2 K zero field Mössbauer spectra of IsnB reaction. The black hashed lines represent spectra of samples freeze quenched at various time points by rapid mixing of IsnB•Fe(II)•2OG•substrate (1: left panel and 2: right panel) with O₂. The red lines, the green lines, the blue lines and the purple lines represent the spectral simulations of the Fe(IV)-oxo species, the isonitrile-Fe(II) complex, the enzyme-substrate complex, and the enzyme-product complex. The black lines represent the overall simulations.

Product distributions for IsnB and AmbI3 reactions with **1**, **2** and **5** were characterized using LC-MS. Analogous to SF-Abs experiment condition, the IsnB (or AmbI3)•Fe(II)•2OG complex was incubated with the substrate anaerobically, and then mixed with equal volume of oxygenated buffer with final concentrations of 0.12 mM enzyme, 0.1 mM Fe(II), 0.5 mM substrate, 1.0 mM 2OG, and ~ 0.5 mM O₂. After 5 minutes, the reactions were subjected to LC-MS. In addition to the desaturated products (**3** for IsnB and **4** for AmbI3), a minor peak corresponding to a hydroxylated **1** (**1**-OH) in both reactions was detected (mass shift of +16, $m/z = 229.1$, Fig. 3a and b). The ratio of **1**-OH to **3** or **4** is ~ 1.0 : 5.6. We reasoned that **1**-OH could originate from either a hydroxylated intermediate prior to decarboxylation (e.g., as in Scheme 1C, pathway *i*) or an off-pathway product generated by quenching of a reactive intermediate, such as a benzylic cation or radical (Scheme 1C, pathway *ii*). To distinguish these possibilities, we carried out the reactions in buffer enriched with ¹⁸O-water (~ 75% of ¹⁸OH₂). In both reactions, the ratio of ¹⁶O/¹⁸O product is larger than 99/1 (Fig. 3b). Thus, the oxygen atom of **1**-OH is likely derived from O₂, which is consistent with OH-rebound pathway. Although this observation disfavors the pathway where quenching of reactive species yields **1**-OH, it cannot distinguish whether **1**-OH is the intermediate used for decarboxylation or a product resulting from residual hydroxylase activity.

To probe whether the hydroxylated species is an on-pathway or an off-pathway product, an amide analog **5** was prepared. By replacing the carboxylate with an amide that cannot easily undergo hydroxylation-induced decarboxylation, we anticipate that the IsnB/AmbI3-catalyzed production of **3/4** would decrease with **5** and the hydroxylated intermediate would accumulate if the hydroxylation/decarboxylation pathway operates. In contrast, if desaturation does not proceed through this pathway, we would not observe increased level of the hydroxylated product. When **5** was incubated with IsnB, **3** was still produced. Additionally, a peak with the m/z value corresponding to hydroxylated **5** (**5**-OH) was detected ($m/z = 228.1$), and the ratio of the **5**-OH to **3** is ~ 1 : 6 (Fig. 3c). In the absence of 2OG, neither **3** nor **5**-OH was formed. When AmbI3 was tested, no obvious substrate consumption and product formation could be detected. Although IsnB can catalyze production of **3** and **5**-OH. The reactivity is only ~ 5% compared to **1**. We speculate that the binding affinity of **5** to IsnB and AmbI3 is very poor. While the LC-MS results suggest that the hydroxylated product likely originates from an OH-rebound pathway, the lack of enhancement of hydroxylated product when **5**

was used indicates that it is likely an off-pathway product during IsnB reaction.

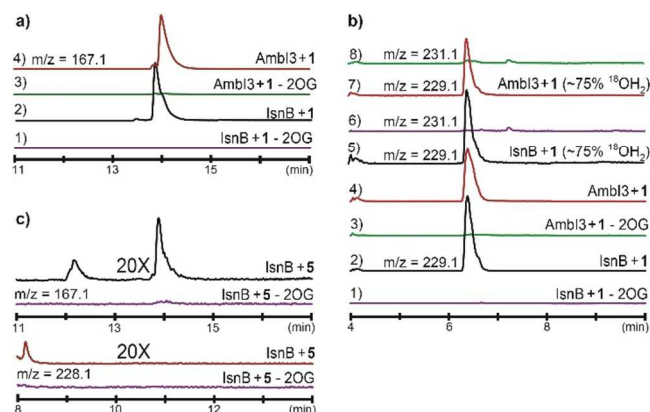


Figure 3: LC-MS analysis of IsnB and AmbI3 catalysis. (a) Formation of **3** and **4** when reacting **1** with IsnB and AmbI3. (b) **1**-OH formation when **1** was reacted with IsnB or AmbI3 (m/z 213.1 \rightarrow 229.1, traces 1-4). In the presence of ~ 75% ¹⁸OH₂, no ¹⁸O incorporation was detected ($m/z = 231.1$, traces 5-8). (c) Formation of **3** and the **5**-OH product (m/z 212.1 \rightarrow 228.1) (top and bottom panels) when **5** was reacted with IsnB. Due to poor reactivity of **5**, traces are enlarged by 20 times (20X).

In conclusion, our results suggest that the catalytic strategy utilizing Fe(IV)-oxo intermediate to trigger benzylic C-H bond activation is operative in IsnB and AmbI3 catalysis. The following steps diverge from the canonical OH-rebound pathway where desaturation is likely to proceed through a pathway involving a benzylic radical or a benzylic carbocation intermediate. An analogous pathway utilizing single electron transfer to the Fe(III)-OH species to produce a substrate cation or a di-radical intermediate has been proposed in the H₂O₂ dependent cytochrome P-450 enzyme, OleT, and O₂ dependent non-heme iron enzyme, UndA,^{15, 16, 22} which imply a common reaction mechanism for decarboxylation-assisted olefination may exist among different types of O₂/H₂O₂ activating enzymes.

ASSOCIATED CONTENT

Supporting Information

The Supporting Information is available free of charge on the ACS Publications website. Methods, Figures S1-S16, Tables S1-S3, and references (PDF)

AUTHOR INFORMATION

Corresponding Author

E-mail: wchang6@ncsu.edu, ysguo@andrew.cmu.edu, xinyuliu@pitt.edu

& These authors contribute equally.

ACKNOWLEDGMENT

This work was supported by grants from North Carolina State University, Carnegie Mellon University, and NSF CHE-1654060 (to Y. G.).

REFERENCES

[1] Tang, M. C., Zou, Y., Watanabe, K., Walsh, C. T., and Tang, Y. (2017) Oxidative Cyclization in Natural Product Biosynthesis, *Chem. Rev.* 117, 5226-5333.

- [2] Martinez, S., and Hausinger, R. P. (2015) Catalytic Mechanisms of Fe(II)- and 2-Oxoglutarate-dependent Oxygenases, *J. Biol. Chem.* *290*, 20702-20711.
- [3] Galonic, D. P., Barr, E. W., Walsh, C. T., Bollinger, J. M., Jr., and Krebs, C. (2007) Two interconverting Fe(IV) intermediates in aliphatic chlorination by the halogenase CytC3, *Nat. Chem. Biol.* *3*, 113-116.
- [4] Matthews, M. L., Krest, C. M., Barr, E. W., Vaillancourt, F. H., Walsh, C. T., Green, M. T., Krebs, C., and Bollinger, J. M. (2009) Substrate-triggered formation and remarkable stability of the C-H bond-cleaving chloroferryl intermediate in the aliphatic halogenase, SyrB2, *Biochemistry* *48*, 4331-4343.
- [5] Mitchell, A. J., Zhu, Q., Maggiolo, A. O., Ananth, N. R., Hillwig, M. L., Liu, X., and Boal, A. K. (2016) Structural basis for halogenation by iron- and 2-oxo-glutarate-dependent enzyme WelO5, *Nat. Chem. Biol.* *12*, 636-640.
- [6] Ishikawa, N., Tanaka, H., Koyama, F., Noguchi, H., Wang, C. C., Hotta, K., and Watanabe, K. (2014) Non-heme dioxygenase catalyzes atypical oxidations of 6,7-bicyclic systems to form the 6,6-quinolone core of viridicatin-type fungal alkaloids, *Angew. Chem. Int. Ed.* *53*, 12880-12884.
- [7] McGowan, S. J., Sebaihia, M., Porter, L. E., Stewart, G. S., Williams, P., Bycroft, B. W., and Salmond, G. P. (1996) Analysis of bacterial carbapenem antibiotic production genes reveals a novel beta-lactam biosynthesis pathway, *Mol. Microbiol.* *22*, 415-426.
- [8] Hashimoto, T., Matsuda, J., and Yamada, Y. (1993) Two-step epoxidation of hyoscyamine to scopolamine is catalyzed by bifunctional hyoscyamine 6 beta-hydroxylase, *FEBS Lett.* *329*, 35-39.
- [9] Yan, W., Song, H., Song, F., Guo, Y., Wu, C. H., Her, A. S., Pu, Y., Wang, S., Naowarajna, N., Weitz, A., Hendrich, M. P., Costello, C. E., Zhang, L., Liu, P., and Zhang, Y. J. (2015) Endoperoxide formation by an alpha-ketoglutarate-dependent mononuclear non-haem iron enzyme, *Nature* *527*, 539-543.
- [10] Martinez, S., and Hausinger, R. P. (2016) Biochemical and Spectroscopic Characterization of the Non-Heme Fe(II)- and 2-Oxoglutarate-Dependent Ethylene-Forming Enzyme from *Pseudomonas syringae* pv. phaseolicola PK2, *Biochemistry* *55*, 5989-5999.
- [11] Brady, S. F., and Clardy, J. (2005) Cloning and heterologous expression of isocyanide biosynthetic genes from environmental DNA, *Angew. Chem. Int. Ed.* *44*, 7063-7065.
- [12] Brady, S. F., and Clardy, J. (2005) Systematic investigation of the *Escherichia coli* metabolome for the biosynthetic origin of an isocyanide carbon atom, *Angew. Chem. Int. Ed.* *44*, 7045-7048.
- [13] Chang, W.-c., Sanyal, D., Huang, J. L., Ittiamornkul, K., Zhu, Q., and Liu, X. (2017) In Vitro Stepwise Reconstitution of Amino Acid Derived Vinyl Isocyanide Biosynthesis: Detection of an Elusive Intermediate, *Org. Lett.* *19*, 1208-1211.
- [14] Zhu, J., Lippa, G. M., Gulick, A. M., and Tipton, P. A. (2015) Examining Reaction Specificity in PvcB, a Source of Diversity in Isonitrile-Containing Natural Products, *Biochemistry* *54*, 2659-2669.
- [15] Grant, J. L., Hsieh, C. H., and Makris, T. M. (2015) Decarboxylation of fatty acids to terminal alkenes by cytochrome P450 compound I, *J. Am. Chem. Soc.* *137*, 4940-4943.
- [16] Rui, Z., Li, X., Zhu, X., Liu, J., Domigan, B., Barr, I., Cate, J. H., and Zhang, W. (2014) Microbial biosynthesis of medium-chain 1-alkenes by a nonheme iron oxidase, *Proc. Natl. Acad. Sci. U.S.A.* *111*, 18237-18242.
- [17] Bruender, N. A., and Bandarian, V. (2016) The Radical S-Adenosyl-L-methionine Enzyme MftC Catalyzes an Oxidative Decarboxylation of the C-Terminus of the MftA Peptide, *Biochemistry* *55*, 2813-2816.
- [18] Pavel, E. G., Zhou, j., Busby, R. W., Gunsior, M., Townsend, C. A., and Solomon, E. I. (1998) Circular Dichroism and Magnetic Circular Dichroism Spectroscopic Studies of the Non-Heme Ferrous Active Site in Clavaminate Synthase and Its Interaction with α -Ketoglutarate Cosubstrate, *J. Am. Chem. Soc.* *120*, 743-753.
- [19] Price, J. C., Barr, E. W., Tirupati, B., Bollinger, J. M., Jr., and Krebs, C. (2003) The first direct characterization of a high-valent iron intermediate in the reaction of an alpha-ketoglutarate-dependent dioxygenase: a high-spin FeIV complex in taurine/alpha-ketoglutarate dioxygenase (TauD) from *Escherichia coli*, *Biochemistry* *42*, 7497-7508.
- [20] Price, J. C., Barr, E. W., Glass, T. E., Krebs, C., and Bollinger, J. M., Jr. (2003) Evidence for hydrogen abstraction from C1 of taurine by the high-spin Fe(IV) intermediate detected during oxygen activation by taurine:alpha-ketoglutarate dioxygenase (TauD), *J. Am. Chem. Soc.* *125*, 13008-13009.
- [21] Chang, W.-c., Guo, Y., Wang, C., Butch, S. E., Rosenzweig, A. C., Boal, A. K., Krebs, C., and Bollinger, J. M., Jr. (2014) Mechanism of the C5 stereoinversion reaction in the biosynthesis of carbapenem antibiotics, *Science* *343*, 1140-1144.
- [22] Grant, J. L., Mitchell, M. E., and Makris, T. M. (2016) Catalytic strategy for carbon-carbon bond scission by the cytochrome P450 OleT, *Proc. Natl. Acad. Sci. U.S.A.* *113*, 10049-10054.

SYNOPSIS TOC (Word Style "SN_Synopsis_TOC").

